ISSN 1063-7761, Journal of Experimental and Theoretical Physics, 2012, Vol. 115, No. 2, pp. 185–193. © Pleiades Publishing, Inc., 2012.
Original Russian Text © P.N. Melentiev, A.E. Afanasiev, A.A. Kuzin, A.V. Zablotskiy, A.S. Baturin, V.I. Balykin, 2012, published in Zhurnal Eksperimental'noi i Teoreticheskoi Fiziki, 2012, Vol. 142, No. 2, pp. 211–221.

ATOMS, MOLECULES, OPTICS

Extremely High Transmission of Light through a Nanohole inside a Photonic Crystal

P. N. Melentiev[a,*], A. E. Afanasiev[a], A. A. Kuzin[b], A. V. Zablotskiy[b], A. S. Baturin[b], and V. I. Balykin[a]

[a] *Institute for Spectroscopy, Russian Academy of Sciences, Troitsk, Moscow, 142190 Russia*

* *e-mail: laser.isan@gmail.com*

[b] *Moscow Institute of Physics and Technology (State University), Dolgoprudnyi, Moscow oblast, 141700 Russia*

Received November 25, 2011

Abstract—The transmission of light through single nanoholes with diameters considerably smaller than the wavelength of light (smaller than $\lambda/10$) is experimentally studied. The nanoholes were made in a gold film, which is a part of a photonic crystal forming a microcavity with the quality factor $Q \approx 100$. A 28-fold increase in the transmission of light through a nanohole inside the microcavity compared to transmission through a nanohole in a gold film is demonstrated. The high spectral selectivity of light transmission through a nanohole is discovered, which is characterized by two features: (i) the transmission maximum is located at the resonance wavelength of the microcavity and (ii) the peak full width at half-maximum is about $\lambda/90$.

DOI: 10.1134/S1063776112070114

1. INTRODUCTION

The phenomenon of transmission of electromagnetic and material de Broglie waves through holes in a screen has always attracted great interest in various fields of physics. The first experiments on the transmission of light through a hole have laid the foundation of classical optics and have numerous practical applications. Studies of the transmission of material particles through a hole have played a noticeable role in proving the wave nature of material particles and the subsequent development of atomic optics [1] and atomic lithography [2]. Holes in a cell membrane in living systems play an important role of a selective filter [3].

One of the key characteristics of particle transmission through a hole is the transmitted particle flux. When the hole size is smaller than the corresponding wavelength, the transmitted flux of particles (both photons and material particles) is very weak, which hinders their applications, making them of little interest. Because of this, the discovery of extraordinary transmission (EOT) [4] has aroused considerable excitement in the scientific community. Numerous subsequent fundamental studies in this field have made the subwavelength hole a new optical element [5]. At present a new class of optical elements based on the EOT effect has been created, which includes light diodes, selective polarization filters, and energy amplifiers. An attempt to implement the extreme transmission of waves of matter has also been proposed [6].

In the case of EOT through a nanohole, the ratio of the energy transmitted through a hole in a screen to the incident energy can exceed unity and exceeds by a few orders of magnitude the ratio predicted by the Bethe theory for subwavelength holes [7–9]. The extremely high transmission of radiation is explained by many factors, one of the main among them being the efficient excitation of surface (plasmon) oscillations [5]. The transmission of light through nanoholes can be also enhanced due to the constructive interference of waves, similarly to the formation of Fabry–Perot resonances [10, 11].

The appearance of the EOT effect (excitation of plasmon waves and Fabry–Perot resonances) and its use in the case of holes is restricted by a number of factors: (i) the necessity of having comparatively large holes with diameters slightly smaller than the diameter corresponding to the cutoff wavelength of the propagating mode in a waveguide formed by the nanohole [12], (ii) the requirement on the high conductivity of the screen material (usually gold and silver); (iii) the necessity of having periodic structures; and (iv) a large resonant spectral width of transmitted radiation.

A separate important problem is the considerable increase in the photon flux through a single nanohole because a single nanohole allows implementation of a spatially localized light source (Fig. 1a) having wide practical applications. By now a maximum increase in the transmission through a single nanohole of $G = 125$ was achieved due to excitation of surface plasmons in concentric indentations surrounding the nanohole and arranged periodically in the radial direction [13]. Among other approaches, a Pendry lens [14] should be mentioned, which is a resonator considerably smaller than the wavelength of light. It was shown in [15] that such a lens mounted in the near-field region of a nanohole provided an approximately 740-fold increase in

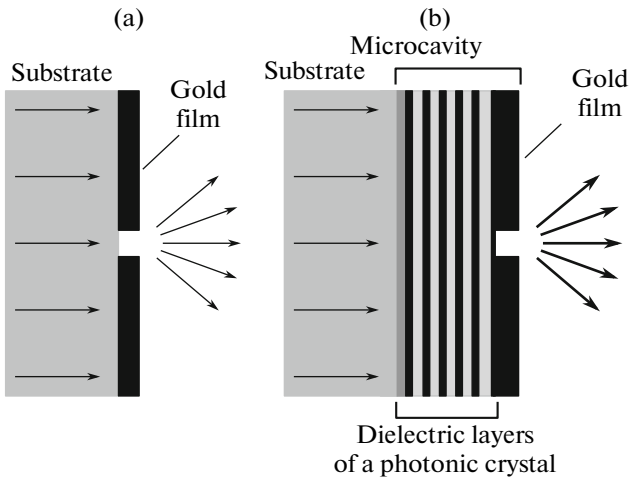

Fig. 1. (a) Nanohole in a gold film deposited on a quartz substrate. (b) Nanohole in a gold film that is a part of a microcavity formed on a quartz substrate using a photonic crystal.

radiation transmission through a single nanohole at electromagnetic field frequencies in the region of a few gigahertz. However, the implementation of this approach in the optical range is restricted by the necessity of controlling the lens size with an accuracy of a few nanometers. In [16], a different mechanism of EOT through single holes was proposed and implemented. The authors of [16] placed a nanohole in a light field localized in a one-dimensional photonic crystal.

Photonic crystals were first proposed more than two decades ago to obtain strong localization of light [17, 18]. Among the variety of micro- and nanoresonators, photonic-crystal-based resonators are one promising device for studying quantum electrodynamic effects, because their Q factor can reach 10^6. The physical properties of a quantum-mechanical system placed in a photonic crystal differ from these of a system in free space. In particular, the spontaneous emission rate can increase, and second harmonic generation and many other effects are possible [17].

It is known that transmission of light through a nanohole can be quite accurately simulated using the Babinet principle, in which a nanohole is replaced by a nanodisk characterized by the corresponding (magnetic and electric) dipole moments, as Bethe did for the first time [7]. It is also well known that the radiative properties of a dipole placed in a resonator differ from these of a dipole in free space. The basic idea of our approach is to create conditions in which a nanohole (effective dipole) is placed in the region of the maximum field of a one-dimensional photonic crystal. In this case, conditions can be obtained under which the emission rate of an effective dipole increases, resulting in a corresponding increase in the light power transmitted through the nanohole.

In this paper, we studied in detail the EOT effect by placing a nanohole with a diameter considerably smaller than the wavelength of light into the field of a microcavity formed by a one-dimensional photonic crystal and a gold film.

2. INCREASE IN THE LIGHT INTENSITY IN A PHOTONIC-CRYSTAL RESONATOR

We used a microcavity based on a one-dimensional photonic crystal. The photonic crystal is formed by 12 alternating dielectric layers with a thickness of $x_i = \lambda/4n_i$, where λ is the emission wavelength (λ = 730 nm) and n_i is the refractive index of a layer material. The dielectric layers are arranged so that a layer with a the high refractive index (TiO_2, $n_{TiO_2} = 2.23$ [19]) is followed by a layer with a low refractive index (MgF_2, $n_{MgF_2} = 1.38$ [19]). The dielectric layers form a one-dimensional photonic crystal providing weak (about 2%) transmission of light in the spectral range from 650 to 800 nm (the forbidden band of the photonic crystal). The dielectric layers with gold layers deposited on them (Fig. 1b) form a microcavity with a Q factor of about 100.

The transmission of a plane light wave through the microcavity was described by means of the characteristic matrix. A change in the light field after transmission through each dielectric layer is determined by a 2×2 matrix, while the influence of all layers is determined by the product of such individual matrices, the so-called characteristic matrix [20]:

$$M = M_1 M_2 \ldots M_{12} M_{Au} = \begin{bmatrix} m_{11} & m_{12} \\ m_{21} & m_{22} \end{bmatrix},$$
$$M_j = \begin{bmatrix} \cos(kh_j) & [i\sin(kh_j)]/Y_j \\ iY_j\sin(kh_j) & \cos(kh_j) \end{bmatrix}. \quad (1)$$

The M_j matrix connects the electric and magnetic components of the light field at the input and output of the microcavity,

$$\begin{bmatrix} E_{in} \\ H_{in} \end{bmatrix} = M_j \begin{bmatrix} E_{out} \\ H_{out} \end{bmatrix}, \quad (2)$$

where $k = 2\pi/\lambda$ is the wave number of the incident wave, $h_j = n_j x_j$ is the optical layer thickness, and $Y_j = \sqrt{\varepsilon_0/\mu_0}\, n_j$. The amplitude reflection coefficient r and amplitude transmission coefficient t are described by the expressions

$$r = \frac{Y_0 m_{11} + Y_0 Y_s m_{12} - m_{21} - Y_s m_{22}}{Y_0 m_{11} + Y_0 Y_s m_{12} + m_{21} + Y_s m_{22}}, \quad (3)$$

$$t = \frac{2Y_0}{Y_0 m_{11} + Y_0 Y_s m_{12} + m_{21} + Y_s m_{22}}. \quad (4)$$

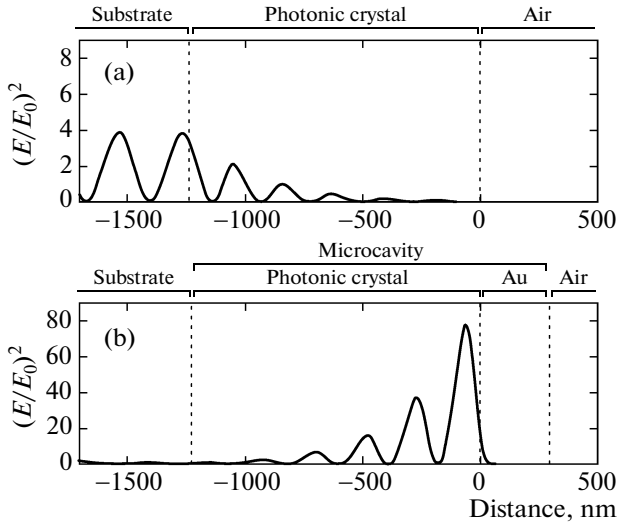

Fig. 2. Spatial electric-field distributions for a light wave in (a) dielectric layers of a photonic crystal and (b) in a microcavity formed by dielectric layers of a photonic crystal and a gold film.

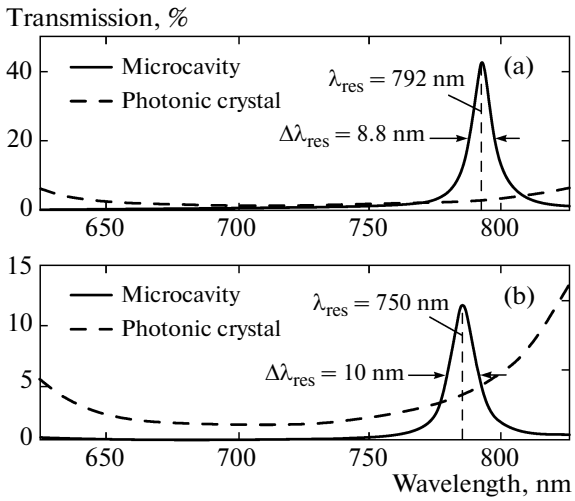

Fig. 3. Transmission spectra of a photonic crystal and the microcavity containing a 45-nm thick gold film: (a) calculated by the characteristic matrix method and (b) measured experimentally.

We considered the propagation of a plane monochromatic wave inside a photonic crystal with the wave vector directed orthogonally to the plane of the dielectric layers. Three cases were studied: (i) A photonic crystal without a gold layer, (ii) a photonic crystal with a 45-nm-thick gold film, and (iii) a a photonic crystal with a 220-nm-thick gold film. In the first case, a microcavity is not formed in a photonic crystal without a gold layer. In the second and third cases, a microcavity is formed with a narrowband mode localized within the forbidden band of the photonic crystal. By decreasing the thickness of the gold layer in the microcavity (second case), we can characterize its resonance mode in transmission. The use of an optically thick gold layer (third case) is necessary for the spatial localization of the resonance mode of the resonator, whose transmission is extremely low because of the strong absorption of light in the gold film.

Figure 2a shows the electric field distribution $E^2(r)$ in the photonic crystal axis at the resonance wavelength $\lambda_{res} = 789.6$ nm of the microcavity calculated using the characteristic matrix and normalized to the square E_0^2 of the field amplitude of the incident plane wave. The electric field distribution inside the microcavity formed by the photonic crystal and the 220-nm-thick gold layer is shown in Fig. 2b. One can see from Fig. 2a that in the photonic crystal formed only by dielectric layers without a gold layer, a plane wave is strongly reflected and the field in a TiO_2 in contact with air is small, about $0.02E_0^2$. By adding a gold layer to the photonic crystal, we obtain a microcavity (Fig. 2) in which the filed at point x_{max} achieves the maximum value $E_{max}^2 \approx 80E_0^2$ (in a TiO_2 layer adjoining the gold film) and is $\sim 14E_0^2$ at the TiO_2/Au interface. The effective length of the microcavity is extremely small and amounts to,

$$L_{eff} = \frac{\int \varepsilon(x)|E(x)|^2 dx}{\varepsilon(x_{max})|E(x_{max})|^2} \approx 0.17\lambda,$$

where $\varepsilon(x)$ is the spatial dependence of the permittivity of the microcavity.

Figure 3a shows the transmission spectra of the microcavity formed by the photonic crystal and the 45-nm thick old layer and the transmission spectrum of the photonic crystal without a gold layer (dashed curve), calculated by the characteristic matrix method. A narrow resonance at $\lambda_{res} = 792$ nm in the transmission spectrum directly proves the formation of a microcavity because transmission without the microcavity would be much smaller than 2% (Fig. 3a). The resonance width is 8.8 nm, corresponding to the microcavity quality factor $Q = \omega/\Delta\omega \approx 90$.

It is impossible to study of spectral characteristics of transmission for the microcavity formed by the photonic crystal and the 220-nm-thick gold film because the 220-nm-thick gold layer strongly absorbs the incident radiation. Figure 4 shows the calculated reflection spectrum of such a microcavity irradiated by a plane wave from the side of dielectric layers. The resonance in the reflection spectrum is located at $\lambda_{res} =$ 789.6 nm and has a width of 6.6 nm, corresponding to the mode of the microcavity with a Q factor of ~120. Despite the moderate value of the microcavity's Q factor, this configuration has a specific property of strong amplification of the light field near the gold film surface, which is important for further applications.

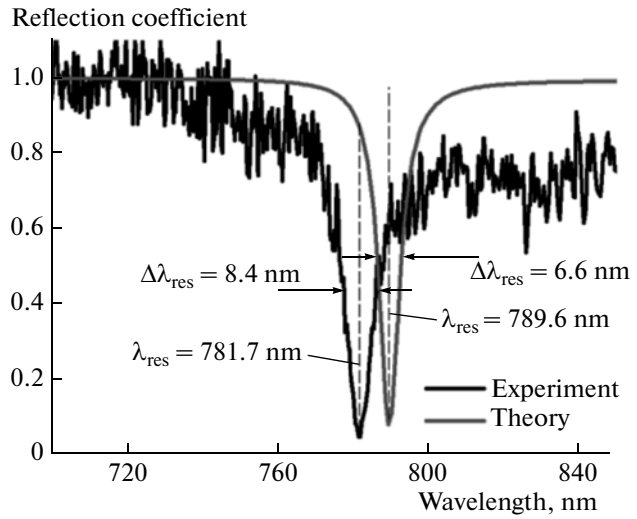

Fig. 4. Reflection spectra of the microcavity in which the last Au layer is 220-nm thick (theory and experiment).

Note some important properties of the chosen microcavity configuration: an Al_2O_3 layer ($n_{Al_2O_3} = 1.63$) located between a quartz substrate and a TiO_2 layer reduces the jump of the refractive index in the light propagation direction and provides an increase in the field amplitude of the resonance mode of the microcavity. The thick gold film strongly reduces the light field, which is necessary for further investigations of transmission of light through nanoholes made in such a gold film.

Dielectric layers in the microcavity were deposited on the surface of a quartz substrate in a high vacuum with ion assistance. The gold film was deposited by thermal sputtering. The microcavity was made in a class 100 clean room. The thickness and roughness of prepared golf films were measured with an atomic force microscope. The measured roughness amplitude (root-mean-square deviation) was about 3 nm, and the longitudinal roughness (correlation length) was about 30 nm.

The experimental transmission spectrum of the microcavity with a partially transmitting 45-nm-thick gold layer is shown in Fig. 3b. The dashed curve in this figure shows the transmission spectrum of the photonic crystal without a gold layer. The experimental reflection spectrum of the microcavity with a 220-nm-thick gold layer is shown in Fig. 4. One can see that after deposition of the gold film on the photonic crystal, a resonance appears in the forbidden band of the crystal transmission, indicating the formation of a microcavity. The measured resonance wavelength of the microcavity with the optically thick gold layer is $\lambda_{res} = 781.7$ nm and the resonance full width at half-maximum is $\Delta\lambda_{res} = 8.4$ nm. The Q factor of this microcavity is 93.

3. PRODUCTION OF NANOHOLES IN THE PHOTONIC-CRYSTAL MICROCAVITY

Nanoholes in a gold layer of the microcavity were produced with a tightly focused ion beam (FEI Quanta 3D ion beam setup with Ga^+ ions at 30 keV with a beam about 10 nm in diameter on a surface). With this ion beam, nanoholes smaller than 100 nm in diameter were fabricated. The nanoholes were observed with a JEOL JSM-7001F electron microscope with a spatial resolution of about 5 nm. To reduce the influence of the carbon deposition on the gold film surface induced by the tightly focused electron beam, the nanoholes were observed at a rather moderate accelerating voltage of 5 keV.

Special attention was devoted to the problem of producing nanoholes in a gold film of the microcavity. In a simplified consideration, a nanohole is produced due the knocking out of one gold atom by one ion from the ion beam. When the exposure time of the gold surface to the ion beam is too long, not only a nanohole is produced in the gold film, but a dielectric layer of the microcavity adjoining the gold film is damaged. This leads to considerable impairment in the characteristics of the microcavity mode. On the other hand, for short exposure times, a through hole cannot be produced in the gold film, which prevents the penetration of the light field localized in the microcavity to the nanohole.

The optimal ion beam exposure was determined in a separate experiment on the production of nanoholes in a gold film deposited on an ultrathin 40-nm-thick SiO_2 film [21]. The use of such a film, first, allowed the control of the ion flux transmitted through a nanohole [22] and, second, provided the electron microscopy of the hole from both sides of the film. The image contrast in an electron microscope is sensitive to the material of an object under study, which makes it possible to identify the SiO_2/Au interface inside a nanohole and to determine the degree of SiO_2 film damage.

A gold layer on the ultrathin SiO_2 film was produced simultaneously with the deposition of gold on a one-dimensional photonic crystal in the manufacture of a microcavity, which ensured the same gold layer thickness in the microcavity and on the SiO_2 film surface. After a series of experiments, we determined the optimal ion-beam dose, which is 4 pC for a focused ion-beam current of 10 pA. An ion beam with such parameters can produce a hole with a diameter ~60 nm in the gold film, the walls of the hole being almost vertical (deviation from the vertical is ~5°). The hole in the SiO_2 film is not through, which suggests that the damage to the SiO_2 film along the hole axis is smaller than 40 nm. It was shown in [23] that, for the same parameters of the ion beam, the etching rate of a TiO_2 film is approximately half the etching rate of a SiO_2 film. Based on these data, we estimate the damage depth of the TiO_2 layer near a nanohole in the microcavity as no more than 20 nm.

We manufactured two samples to study the influence of the microcavity on the optical properties of nanoholes in the gold layer of the microcavity (Fig. 1b) and in the reference gold film deposited on a 2-mm thick SiO_2 substrate (Fig. 1a). The thickness of the reference gold film was equal to that of the gold layer in the microcavity. The 10×10 arrays of identical holes were fabricated by the ion beam with parameters indicated above. The distance between nanoholes is 2 μm (Fig. 5a). The inset to Fig. 5a shows the electron-microscope image of one of the holes in the array. Analysis of the images showed that there is a small spread in the sizes and geometries of fabricated nanoholes: (a) about 60% of the holes have a circular shape and diameter of 58 ± 5 nm, (b) a part of the holes have an elliptical shape with the maximum axes $2a = 54$ nm and $2b = 63$ nm. The spread in the size and geometry of nanoholes is caused by the surface inhomogeneity of the gold film deposited by the thermal evaporation method on the dielectric surface. Gold films produced by this method contain nanocrystals formed due to the high surface energy of gold atoms [24].

To study the influence of the diameter of a nanohole on its transmission, we also made nanoholes in both samples at a larger dose of the ion beam of 5 pC at a current of 10 pA. For such ion-beam parameters, the diameter of nanoholes was 72 ± 5 nm (Fig. 5b). For such nanoholes, the damage depth of a TiO_2 layer adjoining the gold layer was estimated as ~25 nm.

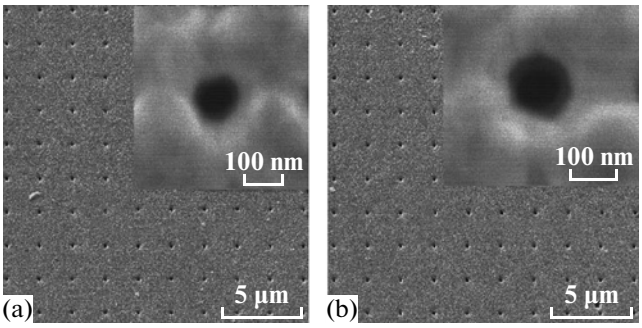

Fig. 5. Electron-microscope images of nanoholes produced in a gold layer of the microcavity by a tightly focused ion beam: (a) holes 60 nm in diameter obtained with the ion beam dose of 4 pC, (b) holes 72 nm in diameter produced with the ion beam dose of 5 pC. The thickness of the gold layer is 220 nm. Insets show the images of individual holes.

4. EXPERIMENTAL SETUP AND THE METHOD FOR MEASURING TRANSMISSION OF LIGHT BY A SINGLE NANOHOLE

The transmission of light by a nanohole produced in a gold film was measured using an optical microscope in the experimental setup shown in Fig. 6. Both samples were irradiated by a light beam from a halogen lamp incident normally on a sample (the beam divergence was ~3°). To obtain uniform illumination of a sample, the light from the halogen lamp was transmitted through a multimode optical fiber. The role of collective effects in the transmission of light through a single nanohole was studied by performing measurements at which the light from the halogen lamp was transmitted through a single-mode fiber and then focused with a 10× objective (NA = 0.3) to a spot about 2 μm in diameter (FWHM) in the nanohole plane, illuminating a single nanohole. Special measures were taken to control the incident light intensity. For this purpose, part of the surface of both samples was free of optical covers. The light transmitted through nanoholes was collected with a 100× immersion Nikon objective (NA = 1.49).

We investigated the spectral characteristics of the transmission of nanoholes. The light transmitted through nanoholes was detected by two methods: (i) using a set of band-pass filters followed by the detection of light with a cooled avalanche-signal-amplification CCD array (Princeton Instruments) and (ii) using a high-aperture-ratio monochromator equipped with a cooled CCD linear array (Princeton Instruments). To obtain the maximum collection efficiency of photons transmitted through a nanohole, an immersion oil was used ($n = 1.515$) at the gold/air interface for both samples.

The experimental setup allowed us to obtain the two-dimensional optical image of a single nanohole with a spatial resolution of about 300 nm. The transmission spectrum of a single nanohole was determined by two methods. In the first case, the transmission of an array with nanoholes was measured with a spectrometer with a resolution of about 0.7 nm and then the obtained spectrum was normalized to the number of nanoholes. In the second case, the image signal of a single nanohole was detected with a CCD array at different transmission wavelengths of the band-pass filters placed in front of the CCD array. In this way, the transmission spectra were obtained with a resolution of about 10 nm.

The transmission of a nanohole was measured from the expression

$$T(\lambda) = \frac{Q_{\mathrm{Em}}(\lambda)}{gI(\lambda)S},$$

where $Q_{\mathrm{Em}}(\lambda)$ is the total photon flux transmitted through a nanohole, g is the light collection efficiency of an objective, $I(\lambda)$ is the incident light efficiency, and S is the nanohole area. To determine the parameter g, it is necessary to know the distribution pattern of light transmitted through the nanohole. In the configuration under study, the length of a channel formed by a hole in a gold film is 3.6 times larger than the hole diameter and light transmitted through the nanohole propagates nonuniformly in space: calculations show that radiation is mainly concentrated within a cone with an angle of 150° [25]. The photon collection

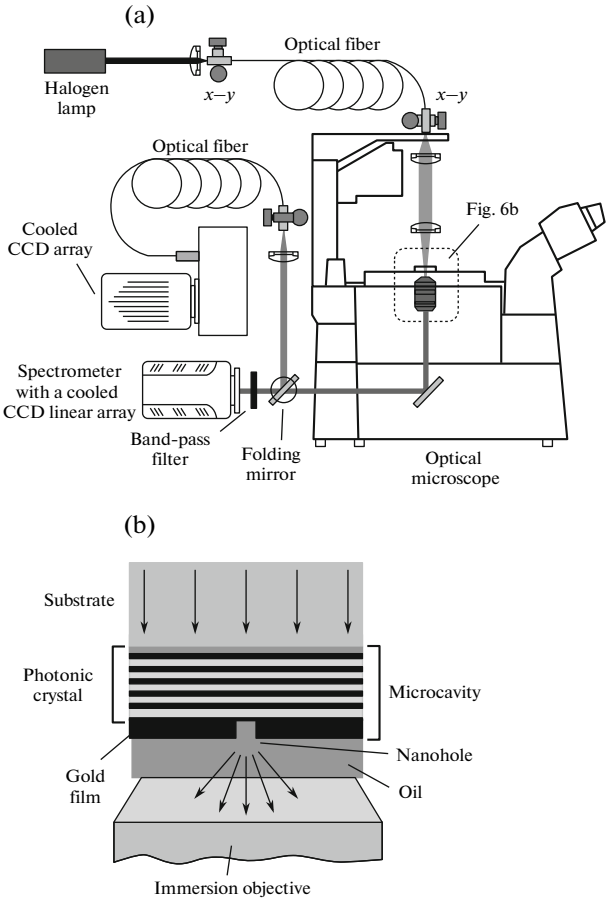

Fig. 6. Scheme of the experimental setup: (a) general scheme and (b) location of the microcavity with a nanohole in a microscope.

angle for an objective with NA = 1.49 is approximately 160°, which allows one to assume that $g \approx 1$.

To avoid errors caused by different spectral sensitivities of different photodetectors and different spectral transmissions of different optical instruments, we measured $I(\lambda)$ in a microscope using the same objective and the same CCD array as for measuring $Q_{Em}(\lambda)$. Note that the density of the photon flux transmitted through a nanohole exceeds by a few orders of magnitude the photon flux density transmitted through a gold film. This allowed us to detect photons actually transmitted through a nanohole against the zero background.

5. TRANSMISSION OF LIGHT BY A NANOHOLE IN THE PHOTONIC-CRYSTAL MICROCAVITY

The transmission of light by a nanohole in the photonic-crystal microcavity was measured with an optical microscope (Fig. 6). Figures 7 and 8 show the images of nanoholes in a reference gold film and nanoholes in the gold microcavity film at a wavelength close to the resonance mode of the microcavity for nanoholes 60 and 72 nm in diameter.

The images of nanoholes for both samples were obtained for the same illumination and probing at a wavelength of $\lambda_c = 780$ nm. For this purpose, a band-pass filter with a transmission wavelength of $\lambda_c = 780$ nm and bandwidth of $\Delta\lambda = 10$ nm was mounted in front of the CCD array. The two-dimensional nanohole images show that the image signal intensity for nanoholes in the reference gold film (Figs. 7a and 8a) is extremely small, whereas the image signal intensity for nanoholes in the microcavity (Figs. 7b and 8b) is extraordinary and exceeds the dynamic range of the signal detection. This means that for the same parameters of the incident radiation, the radiation flux transmitted through nanoholes made in the microcavity is considerably higher than the flux transmitted through nanoholes in the reference gold film. This directly proves that the microcavity increases the transmission of nanoholes.

Figures 7 and 8 show that the transmission of nanoholes produced both in the microcavity and in the reference gold film varies from hole to hole. This difference for some holes achieves 100%. Such a strong variation in the transmitted light intensity cannot be explained only by the known dependence of the transmission of nanoholes on their shape, diameters, and geometry [26].

By analyzing the electron-microscope nanohole images, we established the unique correspondence between the radiation power transmitted through each individual nanohole (Figs. 7 and 8) and its size and geometry. We found that the signal amplitude transmitted through circular nanoholes 60 nm in diameter (Fig. 7) in the reference film was 3.5 relative units, whereas for nanoholes in the microcavity, the corresponding value was 65. The center of the transmission band of the band-pass filter is shifted with respect to the microcavity resonance. Considering this fact, we obtain the correction coefficient 1.53 to the ratio of transmitted powers. Finally, we find that the photon flux transmitted through a nanohole in the microcavity is approximately 28 times higher than the photon flux transmitted through nanoholes in the reference gold film at the resonance wavelength of the microcavity.

One can see from Figs. 7 and 8 that the transmission of nanoholes with different diameters in the microcavity at its resonance wavelength is approximately the same. At the same time, the amplitudes of the transmission signal of nanoholes with different diameters made in the reference gold film differ approximately twice, in good agreement with the Bethe transmission theory, according to which the transmission of a single hole with a diameter considerably smaller than the wavelength of light is proportional to $(d/\lambda)^4$, where d is the nanohole diameter. Our measurements showed that the photon flux reemitted by a nanohole 72 nm in diameter in the microcavity

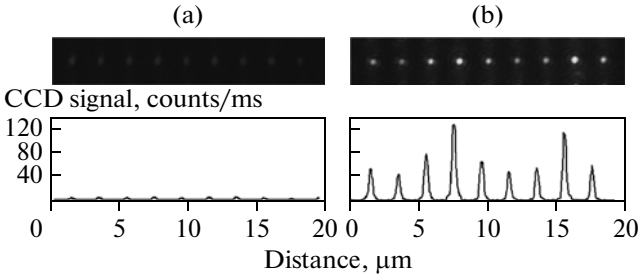

Fig. 7. Optical-microscope images of nanoholes 60 nm in diameter illuminated by white light through a band-pass filter with the transmission band maximum at 780 nm and bandwidth of 10 nm. Two-dimensional images and their transverse profiles for nanoholes in (a) a reference gold film and (b) a gold film in the microcavity.

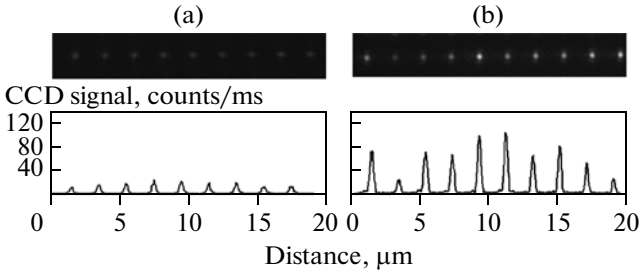

Fig. 8. Optical-microscope images of nanoholes 72 nm in diameter illuminated by white light through a band-pass filter with the transmission band maximum at 780 nm and bandwidth of 10 nm. Two-dimensional images and their transverse profiles for nanoholes in (a) the reference gold film and (b) a gold film in the microcavity.

was approximately 15 times higher than the photon flux transmitted through a similar hole made in the gold film, and this value is approximately half the value for nanoholes 60 nm in diameter.

The measurements of the transmission of holes 60 and 72 nm in diameter in the reference gold film show that the increase in the nanohole transmission with its increasing diameter is consistent with the Bethe theory. The increase in the transmission of nanoholes in the gold layer of the microcavity is explained by the increase in the light field in the microcavity in the region of the nanohole. At the same time, nanoholes can affect the properties of the microcavity, and a correct consideration assumes the study of the microcavity and a nanohole as a single system in which the nanohole transmission no longer satisfies the Bethe theory and is determined by the following basic processes: (i) the amplification of the light field in the microcavity, (ii) the transmission of light through the nanohole, (iii) the change in the parameters of the resonance mode of the microcavity caused by the nanohole, and (iv) the influence of the microcavity on the transmission of light through the nanohole.

The collective influence of nanoholes on their transmission was investigated separately. We used two illumination regimes (at the wavelength of the resonance mode of the microcavity): (i) illumination of all 10×10 nanoholes in the microcavity and reference gold film and (ii) illumination of a single nanohole by tightly focused radiation. The transmission of a single circular nanohole 60 nm in diameter was measured at $T_1 \approx 1.5\%$ in the reference gold film and $T_2 \approx 41\%$ in the microcavity. These values were independent of the illumination regime. Thus, we did not find a collective influence of nanoholes on their transmission, and therefore the total transmission of a nanohole array is equivalent to the total transmission of the same amount of isolated nanoholes.

6. SPECTRAL CHARACTERISTICS OF THE TRANSMISSION OF LIGHT BY A SINGLE NANOHOLE

The characteristic difference of the transmission spectrum of a nanohole in a microcavity from that of a nanohole in a reference film is its sharp frequency selectivity. Figure 9a shows the transmission spectra of single nanoholes 60 and 72 nm in diameter in the reference gold film and microcavity. The transmission spectra of nanoholes in the microcavity exhibit a resonance at the wavelength of the microcavity mode. The resonance width is 9 nm for both nanoholes and corresponds to the spectral width of the microcavity mode. The transmission of a nanohole in the microcavity at wavelengths outside the resonance is determined by the transmission of dielectric layers in the photonic crystal (the forbidden band of the photonic crystal) and is considerably lower than the transmission of nanoholes in the reference gold film. The maximum transmission of a nanohole (60 nm in diameter) in the microcavity achieved at a wavelength of 675 nm is 1.1×10^{-3}, which is almost 300 times smaller than the transmission of this hole at the resonance frequency. Thus, the use of the microcavity provides high spectral selectivity of transmission of a single nanohole.

It is known that localized and propagating surface plasmon waves can strongly change the transmission of light through a nanohole made in metal films by enhancing or attenuating radiation transmitted through the nanohole. We compared the transmission of nanoholes in the gold film of the microcavity with the transmission of the same nanoholes in a gold film prepared on a quartz substrate. Plasmon waves are excited both in the reference gold film and the gold film in the microcavity, and if they contribute to the transmission of light through nanoholes, this contribution should be the same in both cases. In addition, two experimental factors confirm that the increase in the transmission of nanoholes measured in experiments can be assigned only to the influence of the res-

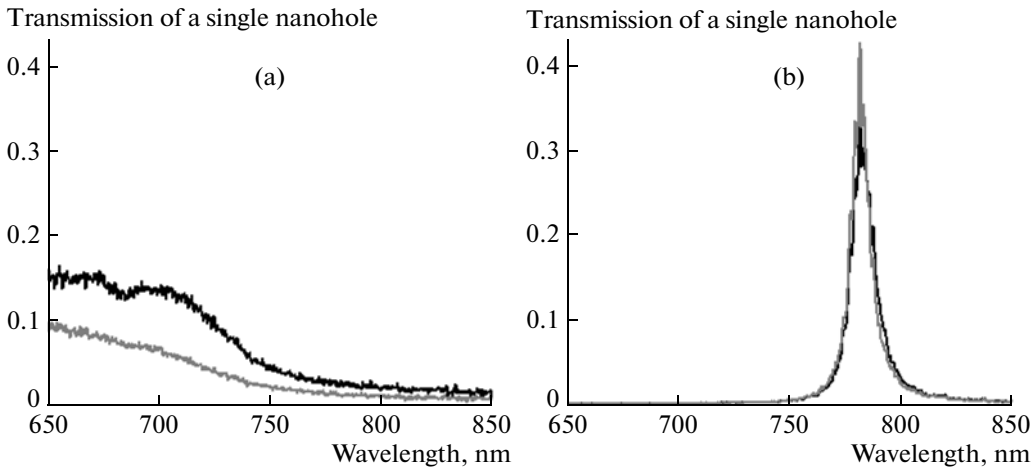

Fig. 9. Transmission spectra of nanoholes with different diameters in (a) the reference gold film and (b) the gold film in the microcavity. Nanoholes 60 nm in diameter (grey curves), nanoholes 72 nm in diameter (black curves).

onance mode of the microcavity. The first factor is the absence of resonances of plasmon waves in experimental transmission spectra on nanoholes in the reference gold film (Fig. 9a), and the second factor is the narrow resonance observed in the transmission of nanoholes in the microcavity with a width considerably smaller than that of plasmon resonances in the transmission spectrum of periodically arranged nanoholes. Effective excitation of plasmon waves in the gold film of the microcavity can additionally increase the transmission of nanoholes in this method.

7. CONCLUSIONS

We have demonstrated the possibility of controlling the transmission of light through a nanohole in a microcavity. We have shown that a nanohole made in a microcavity can, first, provide an increase in transmission at the resonance wavelength of the microcavity and, second, suppress transmission in the forbidden band of a photonic crystal. This method for increasing the transmission of light through a nanohole can be applied in nanolithography using light nanofields [27], quantum informatics [28], sensitometry, data storage [29], second and third harmonic generation [13], and nanosize optical microscopy.

ACKNOWLEDGMENTS

This work was partially supported by the Russian Foundation for Basic Research (grant nos. 11-02-00804-a and 09-02-01022-a) and the "Extreme Light Fields" Program of the Presidium of the Russian Academy of Sciences. The work was performed using the equipment of the Collective Use Centers at the Institute of Spectroscopy, Russian Academy of Sciences, Moscow Institute of Physics and Technology, and Nanotechnology Scientific and Educational Center.

REFERENCES

1. C. E. Wieman, D. J. Wineland, and D. E. Pritchard, Rev. Mod. Phys. **71**, S253 (1999).
2. V. I. Balykin, Phys.—Usp. **52** (3), 275 (2009).
3. B. Alberts, A. Johnson, J. Lewis, M. Raff, K. Roberts, and P. Walter, *Molecular Biology of the Cell* (Garland Science, New York, 2002).
4. T. W. Ebbesen, H. J. Lezec, H. F. Ghaemi, T. Thio, and P. A. Wolff, Nature (London) **391**, 667 (1998).
5. F. J. Garcia-Vidal, L. Martin-Moreno, T. W. Ebbesen, and L. Kuipers, Rev. Mod. Phys. **82**, 729 (2010).
6. E. Moreno, A. I. Fernandez-Dominguez, J. I. Cirac, F. J. Garcia-Vidal, and L. Martin-Moreno, Phys. Rev. Lett. **95**, 170406 (2005).
7. H. A. Bethe, Phys. Rev. **66**, 163 (1944).
8. C. J. Bouwkamp, *Diffraction Theory* (Physical Society, London, 1954).
9. F. J. Garcá de Abajo, Rev. Mod. Phys. **79**, 1267 (2007).
10. A. Krishnan, T. Thio, T. J. Kim, H. J. Lezec, T. W. Ebbesen, P. A. Wolff, J. Pendry, L. Martín-Moreno, and F. J. García-Vidal, Opt. Commun. **200**, 1 (2001).
11. F. Kalkum, M. Peter, G. Barbastathis, and K. Buse, Appl. Phys. B **100**, 169 (2010).
12. E. Popov and N. Bonod, in *Structured Surfaces as Optical Metamaterials*, Ed. by A. A. Maradudin (Cambridge University Press, Cambridge, 2011), p. 1.
13. A. Nahata, R. A. Linke, T. Ishi, and K. Ohashi, Opt. Lett. **28**, 423 (2003).
14. J. B. Pendry, A. J. Holden, D. J. Robbins, and W. J. Stewart, IEEE Trans. Microwave Theory Tech. **47**, 2075 (1999).
15. K. Aydin, A. Cakmak, L. Sahin, Z. Li, F. Bilotti, L. Vegni, and E. Ozbay, Phys. Rev. Lett. **102**, 013904 (2009).
16. P. N. Melentiev, A. E. Afanasiev, A. A. Kuzin, A. V. Zablotskiy, A. S. Baturin, and V. I. Balykin, Opt. Express **19**, 22743 (2011).
17. E. Yablonovich, Phys. Rev. Lett. **58**, 2059 (1987).

18. S. John, Phys. Rev. Lett. **58**, 2486 (1987).
19. I. Ya. Bubis, V. A. Veidenbakh, I. I. Dukhopel, V. G. Zubakov, S. S. Kachkin, S. M. Kuznetsov, Yu. V. Lisitsyn, M. A. Okatov, G. T. Petrovskii, G. D. Pridatko, L. V. Sergeev, V. I. Smirnov, N. V. Suikovskaya, I. D. Torbin, and B. A. Chunin, *Handbook of Technologist–Optician*, Ed. by S. M. Kuznetsov and M. A. Okatov (Mashinostroenie, Leningrad, 1983) [in Russian].
20. M. Born and E. Wolf, *Principles of Optics: Electromagnetic Theory of Propagation, Interference, and Diffraction of Light* (Pergamon, London, 1959; Nauka, Moscow, 1973).
21. P. N. Melentiev, A. V. Zablotskiy, D. A. Lapshin, E. P. Sheshin, A. S. Baturin, and V. I. Balykin, Nanotechnology **20**, 235301 (2009).
22. D. P. Adams, M. J. Vasile, V. Hodges, and N. Patterson, Microsc. Microanal. **13**, 1512 (2007).
23. D. R. Baer, M. H. Engelhard, A. S. Lea, P. Nachimuthu, T. C. Droubay, J. Kim, B. Lee, C. Mathews, R. L. Opila, L. V. Saraf, W. F. Stickle, R. M. Wallace, and B. S. Wright, J. Vac. Sci. Technol., A **28**, 1060 (2010).
24. D. W. Pashley, M. J. Stowell, M. H. Jacobs, and T. J. Law, Philos. Mag. **10**, 127 (1964).
25. J. D. Jackson, *Classical Electrodynamics* (Wiley, New York, 1962; Mir, Moscow, 1965).
26. K. J. Klein Koerkamp, S. Enoch, F. B. Segerink, N. F. van Hulst, and L. Kuipers, Phys. Rev. Lett. **92**, 183901 (2004).
27. V. I. Balykin, V. V. Klimov, and V. S. Letokhov, in *Handbook of Theoretical and Computational Nanotechnology*, Ed. by M. Rieth and W. Schommers (Elsevier, Amsterdam, The Netherlands, 2006), p. 1.
28. E. Altewischer, M. P. van Exter, and J. P. Woerdman, Nature (London) **418**, 304 (2002).
29. J. Vučković, M. Loncar, and A. Scherer, IEEE J. Quantum Electron. **36**, 1131 (2000).

Translated by M. Sapozhnikov